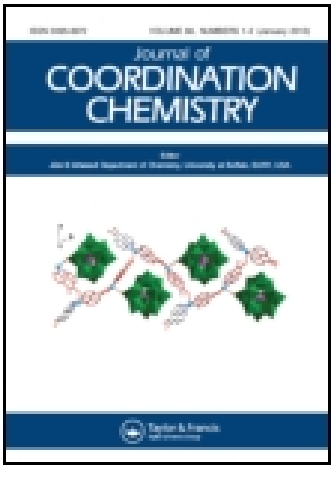

Journal of Coordination Chemistry
Publication details, including instructions for authors and subscription information:
http://www.tandfonline.com/loi/gcoo20

Synthesis, crystal structure, solid-state fluorescence, and interaction with DNA of mononuclear La(III) complex: $La(Phen)_2L_2(NO_3)$

En-Jun Gao[a], Quan Yao[a], Ming-Chang Zhu[a], Dong Zhang[a], Mei-Yu Li[a], Hong Fu[a], Mei-Ping Jiang[a], He-Li Yan[a], Xiao-Ying Xun[a], Lin Zhan[a] & Han Wang[a]

[a] International Key Laboratory of Shenyang Inorganic Molecule-based Chemical, Department of Coordination Chemistry, Shenyang University of Chemical Technology, Shenyang, China

Accepted author version posted online: 16 Jun 2014.Published online: 16 Jul 2014.

To cite this article: En-Jun Gao, Quan Yao, Ming-Chang Zhu, Dong Zhang, Mei-Yu Li, Hong Fu, Mei-Ping Jiang, He-Li Yan, Xiao-Ying Xun, Lin Zhan & Han Wang (2014) Synthesis, crystal structure, solid-state fluorescence, and interaction with DNA of mononuclear La(III) complex: $La(Phen)_2L_2(NO_3)$, Journal of Coordination Chemistry, 67:12, 2086-2095, DOI: 10.1080/00958972.2014.935354

To link to this article: http://dx.doi.org/10.1080/00958972.2014.935354

Journal of Coordination Chemistry, 2014
Vol. 67, No. 12, 2086–2095, http://dx.doi.org/10.1080/00958972.2014.935354

Synthesis, crystal structure, solid-state fluorescence, and interaction with DNA of mononuclear La(III) complex: La $(Phen)_2L_2(NO_3)$

EN-JUN GAO*, QUAN YAO, MING-CHANG ZHU, DONG ZHANG, MEI-YU LI, HONG FU, MEI-PING JIANG, HE-LI YAN, XIAO-YING XUN, LIN ZHAN and HAN WANG

International Key Laboratory of Shenyang Inorganic Molecule-based Chemical, Department of Coordination Chemistry, Shenyang University of Chemical Technology, Shenyang, China

(*Received 17 September 2013; accepted 4 May 2014*)

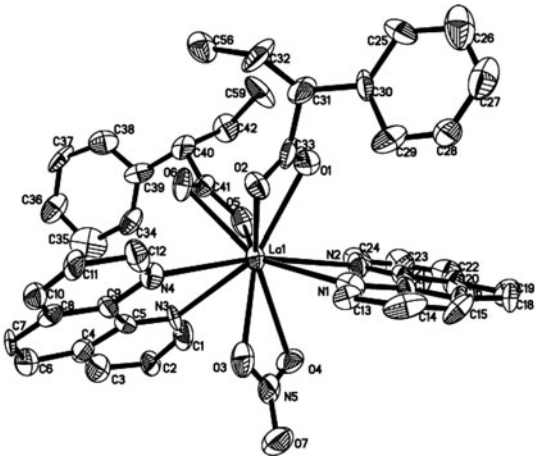

La atom allows the formation of a 10-coordinate distorted-triangle tetrakaidecahedron geometry in the complex.

A mononuclear complex, $La(Phen)_2L_2(NO_3)$ (Phen = 1,10-phenanthroline, L = 2-ethylphenylacetic acid), was synthesized by the reaction of $La(NO_3)_3{\cdot}H_2O$, Phen and L at room temperature. The central ion shows 10-coordination with two Phen and two L molecules. Elemental analysis, IR spectra, and X-ray single-crystal diffraction were carried out to determine the composition and crystal structure. Solid fluorescence shows the luminescent properties of the complex. DNA-binding properties of the complex were examined by fluorescence spectra. The capability of cleavage of pBR322 DNA by the complex was investigated by agarose gel electrophoresis, showing cleaving efficiency.

Keywords: Lanthanum complex; DNA; Gel electrophoresis

*Corresponding author. Email: enjungao@163.com

1. Introduction

Construction of organic–inorganic hybrid materials and/or transition metal coordination polymers have received much attention [1–4]. Coordination architectures, such as polycatenane, polyrotaxane, polythreading, polyknotting, molecular braid, borromean ring, and other unusual structural patterns, with d^{10} and lanthanide metals have been investigated for fluorescence and DNA-cleaving properties for applications in chemical sensors, photochemistry, light emitting diodes, and medicine [5–11].

Recently, a two-ligand assembly system has been used for the construction of new complexes for its tunability of structural frameworks [12, 13]. However, the complexity of the resulting structures caused difficult prediction, and the influential principles in the two-ligand system are still inconclusive. In this work, we choose L(2-ethyl-phenylacetic acid) as the main ligand and Phen as the secondary ligand. $La(Phen)_2L_2(NO_3)$ (**1**) is structurally characterized by elemental analysis, IR, and X-ray crystallography. Crystal structures and systematic investigation of the effect factors in the synthetic process are represented and discussed. The fluorescent and DNA-cleavage properties of the complexes are also discussed.

2. Experimental

2.1. *Chemical reagents and methods*

$La(NO_3)_3{\cdot}H_2O$, Phen, and 2-ethyl-phenylacetic acid were purchased as reagent grade and used without purification. Elemental analyses (C, H, and N) were performed on a Finnigan EA 1112 instrument. IR spectra were recorded on a Nicolet IR-470 spectrophotometer using KBr pellets. Fluorescence was performed on a Perkin–Elmer LS55 fluorescence spectrofluorometer.

2.2. *Synthesis of 1*

Phen and 2-ethyl-phenylacetic acid (0.15 mM) were dissolved in ethanol (10 mL), respectively. A dark pink precipitate appeared when mixing the above-mentioned solution and $La(NO_3)_3{\cdot}H_2O$, with stirring. A KOH solution (0.5 M) was added to adjust the pH until the turbid solution became clear. About 30 mL of the clear solution was kept at room temperature (about 20 °C) and dark pink single crystals were collected two months later. Yield: 61%. Anal. Calcd (%) for the complex $C_{44}H_{40}N_5O_7La$: C, 59.40; H, 4.53; N, 7.87. Found (%): C, 59.48; H, 4.47; N, 7.82. IR (cm^{-1}): 3382m, 3067m, 2933w, 2627s, 2360w, 1822w, 1628s, 1576s, 1453s, 1397s, 1269m,1158s, 933w, 843w, 717s, 685m cm^{-1}.

2.3. *X-ray diffraction analysis*

The crystal structure of **1** was determined by X-ray single-crystal diffraction. The suitable single crystal was mounted in a glass fiber capillary. Data were collected on a Bruker Smart 100 CCD X-ray single-crystal diffractometer with MoKα radiation ($\lambda = 0.71073$ Å) at 293 (2) K in the ω-scan mode. The structure was solved by direct methods using the SHELXL-97 programs [14, 15] and refined by full-matrix least-squares on F^2. All non-hydrogen

atoms were refined anisotropically. Hydrogens were located from difference Fourier maps. Crystal data and structure refinement are summarized in table 1; selected bond distances and angles are provided in table 2.

2.4. *Fluorescence spectroscopic studies*

Ethidium bromide (EtBr) is a planar molecule and it was shown to emit intense fluorescence in the presence of DNA due to its strong intercalation between adjacent DNA base pairs and EtBr. It was previously reported that quenching of DNA–EtBr fluorescence by the addition of complexes causes a reduction in the emission intensity, indicating competition between the complex and EtBr in binding to DNA [16–18]. The quenching extent of fluorescence of EtBr–DNA is used to determine the extent of binding between the complex and the DNA [19].

2.5. *Agarose gel electrophoresis*

The complex as a DNA cleavage agent was examined using supercoiled pBR322 plasmid DNA as the target. The efficiency of cleavage was probed using agarose gel electrophoresis [20–22]. For the gel electrophoresis experiment, pBR322 plasmid DNA (0.5 mg/mL) was treated with **1** dissolved in DMF in Tris buffer (50 mM Tris-acetate, 18 mM NaCl buffer, pH 7.2) and the content was incubated for 1 h at room temperature. The sample was electrophoresed for 1 h at 120 V on 0.8% agarose gel in Tris-acetate buffer. After electrophoresis, the gel was stained with 1 mg/mL EtBr and photographed under UV light [23, 24].

Table 1. Crystallographic data and details of the experiment and refinement of **1**.

Parameter	Value
Empirical formula	$C_{44}H_{40}N_5O_7La$
Formula weight (g M^{-1})	889.72
Crystal system	Monoclinic
Space group	*Cc*
Unit cell dimensions	
a (Å)	13.6303(18)
b (Å)	17.049(2)
c (Å)	16.966(2)
β (°)	97.285(2)
V (Å^3)	3910.78(83)
Z	4
ρ_{Calcd} (g cm^{-3})	3.55341
F (0 0 0)	1808
θ Range for data collection (°)	$1.92 < \theta < 26.05$
Limiting indices	$-13 \le h \le 16$, $-20 \le k \le 21$, $-20 \le l \le 20$
Reflections collected/unique	12,353/6898 ($R_{int} = 0.0339$)
Number of refined parameters	237
Completeness (%)	99.8
Goodness-of-fit on F^2	1.025
Final *R* indices [$I > 2\sigma(I)$]	$R_1 = 0.0493$, $wR_2 = 0.0962$
R indices (all data)	$R_1 = 0.0706$, $wR_2 = 0.1051$
Largest diffraction peak and hole, e^{-3}	1.287 and −0.328

Table 2. Selected bond distances (Å) and angles (°) for **1**.

Bond	*d* (Å)	Bond	*d* (Å)
La(1)–O(5)	2.510 (15)	La(1)–O(1)	2.551 (15)
La(1)–O(2)	2.560 (12)	La(1)–O(6)	2.613 (15)
La(1)–O(3)	2.655 (14)	La(1)–O(4)	2.676 (11)
La(1)–N(1)	2.692 (14)	La(1)–N(4)	2.714 (17)
La(1)–N(3)	2.715 (11)	La(1)–N(2)	2.770 (17)
Angle	*ω* (°)	Angle	*ω* (°)
O(2)–La(1)–O(5)	120.12 (0.17)	O(1)–La(1)–O(5)	82.76 (0.49)
O(6)–La(1)–O(5)	53.13	O(3)–La(1)–O(5)	137.56 (0.46)
O(4)–La(1)–O(5)	99.80 (0.53)	N(1)–La(1)–O(5)	133.76 (0.47)
N(4)–La(1)–O(5)	113.03 (0.49)	N(3)–La(1)–O(5)	72.95 (0.44)
N(2)–La(1)–O(5)	74.18 (0.53)	C(41)–La(1)–O(5)	28.11 (0.48)
C(33)–La(1)–O(5)	103.21 (0.55)	O(1)–La(1)–O(2)	48.75 (0.44)
O(6)–La(1)–O(2)	79.66 (0.45)	O(3)–La(1)–O(2)	100.23 (0.43)
O(4)–La(1)–O(2)	137.79 (0.45)	N(1)–La(1)–O(2)	72.50 (0.42)
N(4)–La(1)–O(2)	74.69 (0.45)	N(3)–La(1)–O(2)	133.04 (0.45)
N(2)–La(1)–O(2)	111.57 (0.47)	C(41)–La(1)–O(2)	97.87 (0.42)
C(33)–La(1)–O(2)	22.83 (0.51)	O(6)–La(1)–O(1)	76.59 (0.16)
O(3)–La(1)–O(1)	138.30 (0.43)	O(4)–La(1)–O(1)	133.58 (0.41)
N(1)–La(1)–O(1)	75.32 (0.47)	N(4)–La(1)–O(1)	118.33 (0.47)
N(3)–La(1)–O(1)	150.45 (0.46)	N(2)–La(1)–O(1)	72.18 (0.49)
C(41)–La(1)–O(1)	76.15 (0.48)	C(33)–La(1)–O(1)	25.92 (0.52)
O(3)–La(1)–O(6)	131.38 (0.40)	O(4)–La(1)–O(6)	140.59 (0.43)
N(1)–La(1)–O(6)	149.24 (0.47)	N(4)–La(1)–O(6)	70.34 (0.48)
N(3)–La(1)–O(6)	75.43 (0.48)	N(2)–La(1)–O(6)	121.11 (0.51)
C(41)–La(1)–O(6)	25.18 (0.41)	C(33)–La(1)–O(6)	77.23 (0.48)
O(4)–La(1)–O(3)	47.61 (0.17)	N(1)–La(1)–O(3)	67.86 (0.39)
N(4)–La(1)–O(3)	63.11 (0.43)	N(3)–La(1)–O(3)	69.82 (0.40)
N(2)–La(1)–O(3)	104.30 (0.46)	C(41)–La(1)–O(3)	143.34 (0.41)
C(33)–La(1)–O(3)	119.14 (0.55)	N(1)–La(1)–O(4)	69.89 (0.40)
N(4)–La(1)–O(4)	103.35 (0.46)	N(3)–La(1)–O(4)	68.65 (0.40)
N(2)–La(1)–O(4)	64.35 (0.48)	C(41)–La(1)–O(4)	124.28 (0.45)
C(33)–La(1)–O(4)	141.66 (0.40)	N(4)–La(1)–N(1)	113.21 (0.46)
N(3)–La(1)–N(1)	133.99 (0.13)	N(2)–La(1)–N(1)	60.56 (0.47)
C(41)–La(1)–N(1)	148.61 (0.47)	C(33)–La(1)–N(1)	72.02 (0.44)

3. Results and discussion

3.1. *X-ray diffraction analysis*

The crystal belongs to the monoclinic system, space group *Cc*, cell parameters: $a = 13.6303(18)°$, $b = 17.049(2)°$, $c = 16.966(2)°$, and $\beta = 97.285(2)°$. In the crystal structure of the lanthanum complex, La forms a ten-coordinate distorted-triangle tetrakaidecahedron geometry with two nitrogens N(1), N(2) from Phen; six carboxylate oxygens O(1), O(2), O(3), O(4), O(5), and O(6) from two 2-ethyl-phenylacetic acid ligands; and a nitrate (figure 1) [25]. The 1-D chain in figure 2 was interconnected by hydrogen bonding between subchains. The 2-D chain structure was interconnected by hydrogen-bonding associations between subchains, which include O(4)···H(56B) and O(3)···H(59B) with bond lengths of 2.686 and 2.673 Å (in the normal ranges), respectively [26–28]. From the depiction in figure 3, the hydrogen bonding plays an important role in the construction of the 2-D structure. Two adjacent 2-D chains interact with each other through π–π stacking interactions between two parallel aromatic rings of Phen, which is further fabricated into the 3-D supramolecular architecture (figure 4). The complex has a polar plane; the nitrate groups clearly align in one direction showing the polarity.

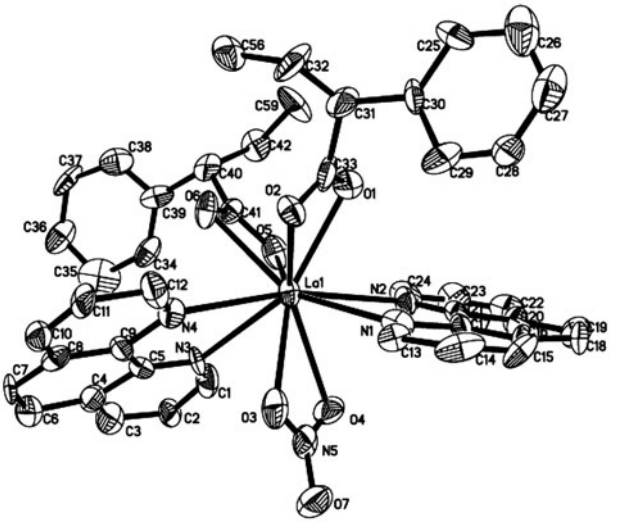

Figure 1. Structure of **1**.

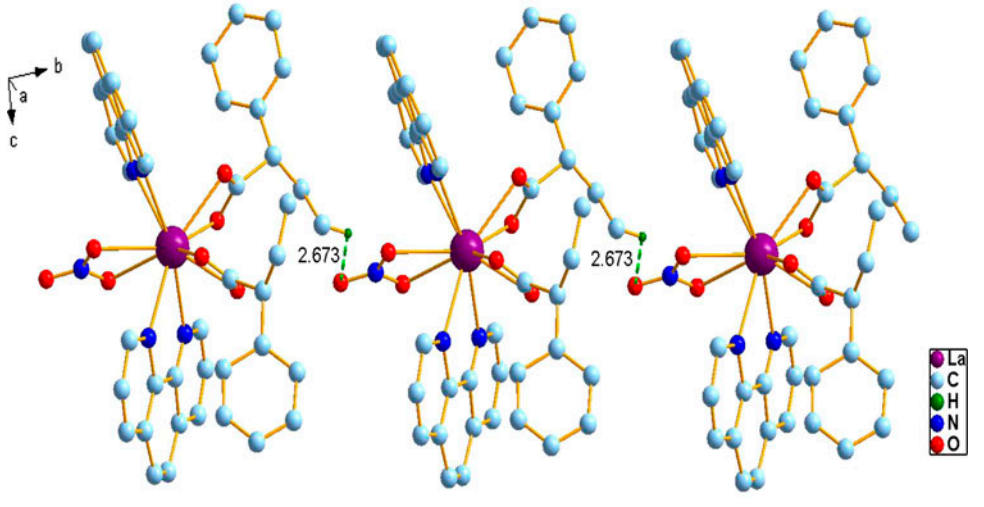

Figure 2. The 1-D structure of **1** formed by hydrogen bonding.

3.2. *Fluorescence spectroscopic studies*

The emission spectrum of EtBr bound to DNA in the absence and presence of **1** is given in figure 5. Addition of the title complex to DNA, pretreated with EtBr, causes reduction in the emission intensity, indicating the replacement of EtBr by **1** [29, 30], consistent with electronic absorption–titration results which indicate that **1** binds to DNA by intercalation, the binding of La(III) complex with DNA linked by four N atoms from two Phen, four O atoms from two 2-ethyl-phenylacetic acid of adjacent purine bases of DNA and form intrastrand cross-links.

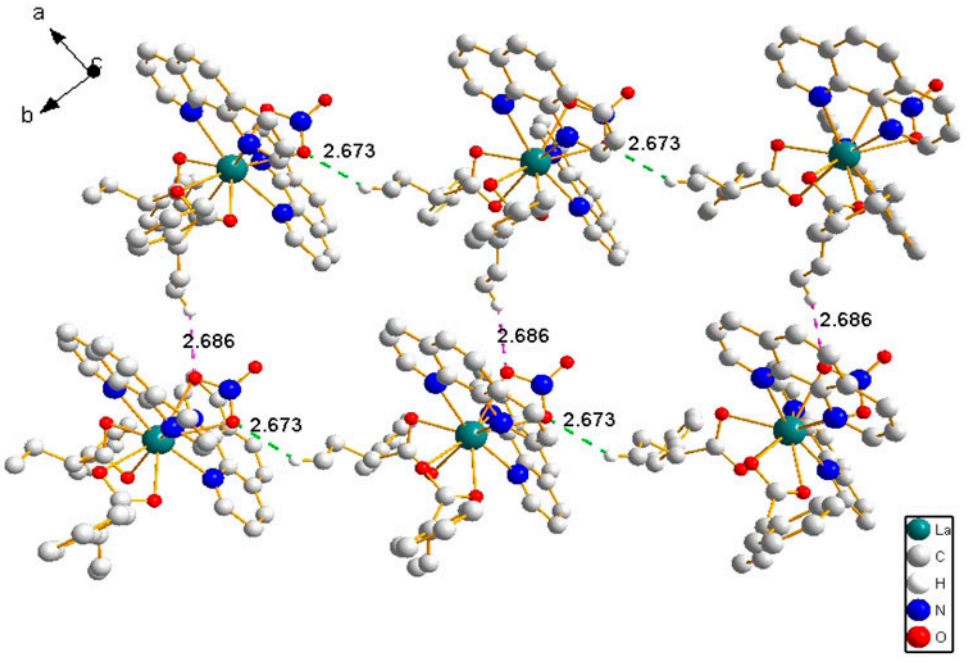

Figure 3. The 2-D structure of **1** formed by two kinds of hydrogen bonding.

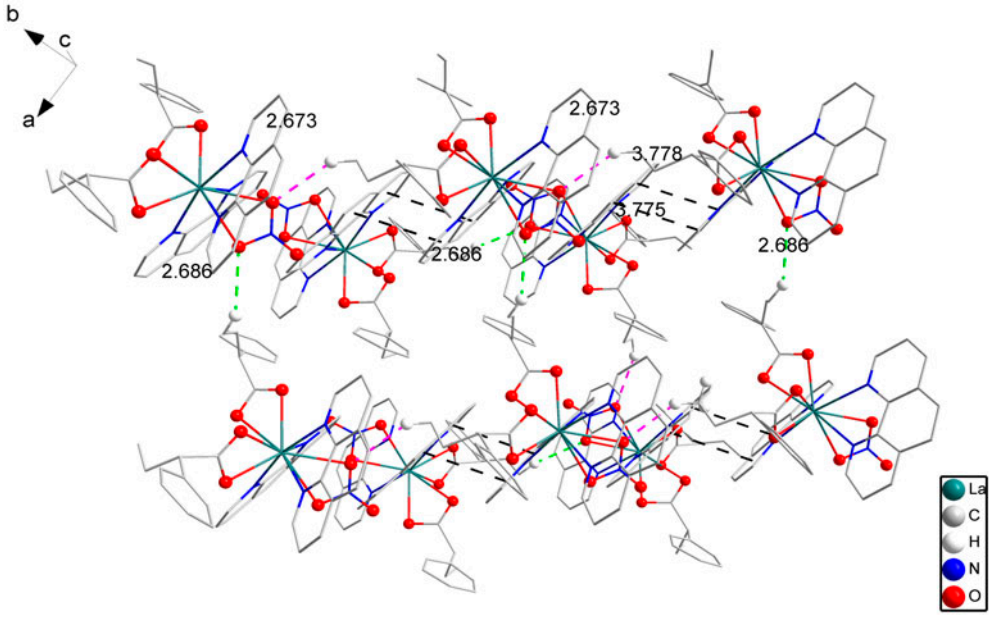

Figure 4. The 3-D structure of **1** by hydrogen bonding and π–π stacking.

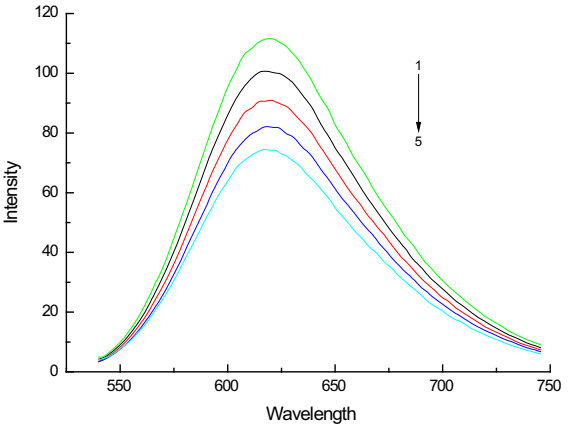

Figure 5. Fluorescence spectra of the binding of EtBr to DNA in the absence (line 1) and presence (lines 2–5) of increasing amount of **1**; $\lambda_{ex} = 617.5$ nm, $C_{EtBr} = 1.0$ μM, and $C_{DNA} = 5.0$ μM.

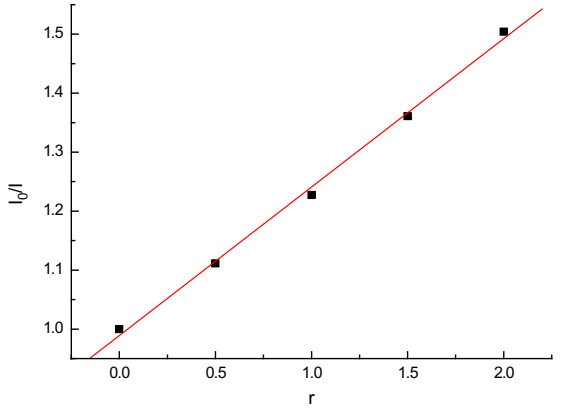

Figure 6. Stern–Volmer quenching plot of **1**.

According to the classical Stern–Volmer equation [31]: $I_0/I = 1 + K_{sq}r$, where I_0 and I represent the fluorescence intensities in the absence and presence of **1**, respectively, r is the concentration ratio of the complex to DNA and K_{sq} is a linear Stern–Volmer quenching constant dependent on the ratio of the bound concentration of EtBr to the concentration of DNA. The K_{sq} value is obtained as the slope of I_0/I *versus* r linear plot. The fluorescence quenching curve of DNA-bound EtBr by **1** is given in figure 6. This complex can be used in molecular fluorescence probe applications.

3.3. *Solid-state fluorescence emission studies*

La(III) complexes exhibit a significant luminous intensity effect [32, 33]. The photoluminescent properties of the complex in the solid state were investigated at room temperature and relevant emission spectra are shown in figure 7. The complex shows an emission centered at 435 nm, upon excitation at 217 nm, which can be assigned to the $\pi \rightarrow \pi^*$

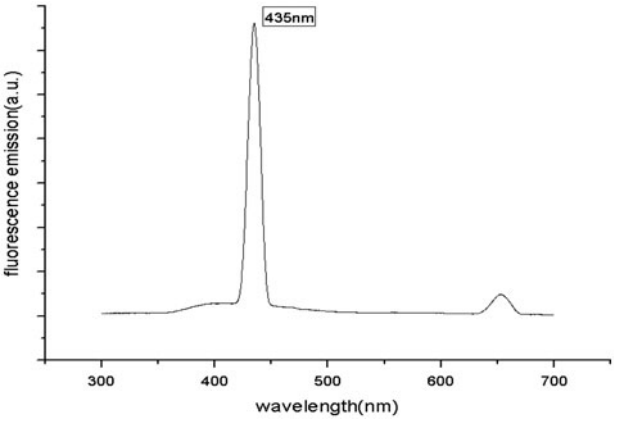

Figure 7. Solid-state fluorescence emission spectra of **1**.

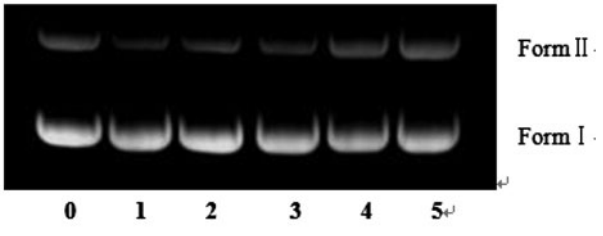

Figure 8. Cleavage of pBR322 DNA (0.5 mg/mL) in the presence of **1**: Lane 0, DNA alone; (lanes 1–5) at different concentrations of complex: (1) 10 mM; (2) 5 mM; (3) 2.5 mM; (4) 1.25 mM; and (5) 0.625 mM.

transitions. Ligand with a rigid aromatic ring and nitrogen containing oxygen atom shuttle aromatic acids, with a large reel of Wu electronic system, and deprotonated carboxyl group, further enhancing the system of reel extent, has maximum absorbance with an absorption coefficient greater than 10^4. Therefore, the fluorescence emission peak of **1** is from π–π* transitions (figure 8).

3.4. *Agarose gel electrophoresis*

Under the effect of external electric field, charged particles move toward its opposite charge on the electrode. In electrophoresis, the sample in the electric field moves with super spiral band (Form I) having low molecular weight and migrates quickly; open-loop tape (Form II) having relatively high molecular weight migrates slowly. **1** has an effect on DNA cutting with greater the concentration, better the cutting results.

4. Conclusion

A mononuclear complex, $La(Phen)_2L_2(NO_3)$ (Phen = 1,10-phenanthroline, L = 2-ethylphenylacetic acid), was synthesized and characterized. The crystal structure of the complex was

determined by single-crystal X-ray diffraction. The DNA binding properties of the complex were examined by fluorescence spectra. The results support the complex binding to DNA by intercalation. Many rare earth complexes also bind to DNA in an intercalative mode, exhibiting strong binding affinity to DNA [34–36]. Solid fluorescence experiments showed that a main emission peak is at 435 nm using an excitation wavelength of 217 nm uv light. The capability of cleavage of pBR322 DNA by **1** was investigated by agarose gel electrophoresis. The results indicate that rare earth-based complexes have practical applications, such as understanding the mechanisms of interaction between small molecules and DNA.

Acknowledgments

We gratefully acknowledge the Natural Science Foundation of China [grant number 21171118], the Distinguished Professor Project of Liaoning Province and the science and technology special fund of Shenyang City (F12-151-9-00).

References

[1] L.A. Borkowski, C.L. Cahill. *Cryst. Growth Des.*, **6**, 2241 (2006).
[2] A.R. Choudhury, T.N. Guru Row. *Cryst. Growth Des.*, **4**, 47 (2004).
[3] S.L. James. *Chem. Soc. Rev.*, **32**, 276 (2003).
[4] N.L. Rosi, M. Eddaoudi, J. Kim, M. O'Keeffe, O.M. Yaghi. *CrystEngComm*, **4**, 401 (2002).
[5] J.L.C. Rowsell, O.M. Yaghi. *Micropor. Mesopor. Mater.*, **73**, 3 (2004).
[6] C.N.R. Rao, S. Natarajan, R. Vaidhyanathan. *Angew. Chem. Int. Ed.*, **43**, 1466 (2004).
[7] Y.F. Han, M. Li, T.W. Wang, Y.Z. Li, Z. Shen, Y. Song, X.Z. You. *Inorg. Chem. Commun.*, **11**, 945 (2008).
[8] M. Eddaoudi, D.B. Moler, H.L. Li, B.L. Chen, T.M. Reineke, M. O'Keeffe, O.M. Yaghi. *Acc. Chem. Res.*, **34**, 319 (2001).
[9] S. Leininger, B. Olenyuk, P.J. Stang. *Chem. Rev.*, **100**, 853 (2000).
[10] L. Pan, H.M. Liu, X.G. Lei, X.Y. Huang, D.H. Olson, N.J. Turro, J. Li. *Angew. Chem. Int. Ed.*, **42**, 542 (2003).
[11] E.J. Gao, M.C. Zhu, H.X. Yin, L. Liu, Q. Wu, Y. Sun. *J. Inorg. Biochem.*, **102**, 1958 (2008).
[12] R.Q. Fan, H. Chen, P. Wang, Y.L. Yang, W. Hasi. *J. Coord. Chem.*, **63**, 1514 (2010).
[13] W.B. Jennings. *Chem. Rev.*, **75**, 307 (1975).
[14] G.M. Sheldrick. *SHELXS-97, Program for Crystal Structure Solution*, University of Göttingen, Germany (1997).
[15] G.M. Sheldrick. *SHELXS-97, Program for Crystal Structure Refinement*, University of Göttingen, Germany (1997).
[16] G.Y. Bai, K.Z. Wang, Z.M. Duan, L.H. Gao. *J. Inorg. Biochem.*, **98**, 1017 (2004).
[17] S.A. Tysoe, R. Kopelman, D. Schelzig. *Inorg. Chem.*, **38**, 5196 (1999).
[18] G.Y. Han, P. Yang. *J. Inorg. Biochem.*, **91**, 230 (2002).
[19] E.J. Gao, K.H. Wang, X.F. Gu, Y. Yu, Y.G. Sun, W.Z. Zhang, H.X. Yin, Q. Wu, M.C. Zhu, X.M. Yan. *J. Inorg. Biochem.*, **101**, 1404 (2007).
[20] B. Macías, M.V. Villa, B. Gómez, J. Borrás, G. Alzuet, M. González-Álvarez, A. Castiñeiras. *J. Inorg. Biochem.*, **101**, 444 (2007).
[21] R.G.M. Moreno, M.V. Alipázaga, O.F. Gomes, E. Linares, M.H.G. Medeiros, N. Coichev. *J. Inorg. Biochem.*, **101**, 866 (2007).
[22] S. Ghosh, A.C. Barve, A.A. Kumbhar, A.S. Kumbhar, V.G. Puranik, P.A. Datar, U.B. Sonawane, R.R. Joshi. *J. Inorg. Biochem.*, **100**, 331 (2006).
[23] E.J. Gao, L. Wang, M.C. Zhu, L. Liu, W.Z. Zhang. *Eur. J. Med. Chem.*, **45**, 311 (2010).
[24] E.J. Gao, M.C. Zhu, Y. Huang, L. Liu, H.Y. Liu, F.C. Liu, S. Ma, C.Y. Shi. *Eur. J. Med. Chem.*, **45**, 1034 (2010).
[25] Y.X. Ren, M.L. Zhang, D.S. Li, F. Fu, J.J. Wang, M. Du, X.Y. Hou, Y.P. Wu. *Inorg. Chem. Commun.*, **14**, 231 (2011).
[26] S.J. Coles, S.E. Durran, M.B. Hursthouse, A.M.Z. Slawin, M.B. Smith. *New J. Chem.*, **25**, 416 (2001).
[27] D. Kovala-Demertzi, J.R. Miller, N. Kourkoumelis, S.K. Hadjikakou, M.A. Demertzis. *Polyhedron*, **18**, 1005 (1999).
[28] P. Li, Y.C. Qiu, J. Liu, Y. Ling, Y. Cai, S. Yue. *Inorg. Chem. Commun.*, **10**, 705 (2007).

[29] H. Mansuri-Torshizi, R. Mital, T.S. Srivastava, H. Parekh, M.P. Chitnis. *J. Inorg. Biochem.*, **44**, 239 (1991).
[30] E.J. Gao, X.M. Zhao, Q.T. Liu, R. Xiu. *Acta Chim. Sin.*, **62**, 593 (2004).
[31] J.R. Lakowicz, G. Weber. *Biochemistry*, **12**, 4161 (1973).
[32] I. Hemmilä, T. Ståhlberg, P. Mottram (Eds.). *Bioanalytical Applications of Labeling Technologies*, Wallac, Turku (1994).
[33] P.G. Avaji, S.A. Patil. *J. Coord. Chem.*, **61**, 2570 (2008).
[34] P. Kapoor, R.V. Singh, N. Fahmi. *J. Coord. Chem.*, **65**, 262 (2012).
[35] M.F. Wang, Z.-Y. Yang, Z.C. Liu, Y. Li, T.R. Li, M.H. Yan, X.Y. Cheng. *J. Coord. Chem.*, **65**, 3805 (2012).
[36] Y.C. Liu, K.J. Zhang, R.X. Lei, J.N. Liu, T.L. Zhou, Z.Y. Yang. *J. Coord. Chem.*, **65**, 2041 (2012).